SCIENTIFIC PAPERS
OF THE UNIVERSITY OF PARDUBICE
Series A
Faculty of Chemical Technology
21 (2015)

SYNTHESIS OF Mg-Al MIXED OXIDES WITH DIFFERENT DISTRIBUTION OF BASIC SITES

Ivana TROPPOVÁ[1], Barbora HUDCOVÁ, Lucie SMOLÁKOVÁ,
and Libor ČAPEK
Department of Physical Chemistry,
The University of Pardubice, CZ–532 10 Pardubice

Received September 25, 2014

The aim of this work is to compare the structure and basicity of Mg-Al mixed oxides with the same Mg/Al molar ratio (Mg/Al 2) synthesised by means of different procedures. We have focused on the preparation of Mg-Al mixed oxides by the thermal pre-treatment of hydrotalcites synthesized by co-precipitation method. The individual methods differed from the application of alkaline solution used to control the reaction pH. We used two solutions, 0.5 M Na_2CO_3 + 3 M NaOH and 2 M NaOH, respectively. Moreover, MgO and two Mg-Al mixed oxides available to large-scale were used to compare the structure and basicity with those of materials synthesized in laboratory. The structure and basicity of Mg-Al mixed oxides were analysed by using XRD, N_2-adsorption, TGA, and TPD-CO_2. As found, the Mg-Al mixed oxide prepared by the thermal pre-treatment of hydrotalcite material and synthesised in the concentrated NaOH solution has exhibited a lower total concentration of basic sites as well as lower relative amount of medium/strong basic sites, in comparison with the Mg-Al mixed oxides originating from the hydrotalcites in the carbonate form.

[1] To whom correspondence should be addressed.

Introduction

Mg-Al mixed oxides represent attractive basic catalysts used, for example, in aldol condensation [1], trans-esterification [2], Michael additions [3], alkylation of phenol [4], Claisen–Schmidt [5], and Knoevenagel condensation[6]. Mg-Al mixed oxides are very often prepared by the thermal pre-treatment of hydrotalcite-like materials [7]. Dehydrogenation, dehydroxylation of hydroxide layers, and decomposition of interlayer carbonate proceed all during the thermal pre-treatment of layered double hydroxide precursors. Surface chemistry and catalytic properties of Mg-Al mixed oxides depend on the process of its synthesis (choice of reagents [8], temperature of the thermal treatment [9]), chemical composition (Mg/Al molar ratio [10]), rehydration [11] and basicity (strength of basic species, their concentration and accessibility [12]).

Generally, hydrotalcite-like layered double hydroxides are natural or synthetic materials with the lamellar structure. Their chemical composition can be expressed by the general formula of $[M^{2+}_{1-x}M^{3+}(OH)_2]^{x+}A^{n-}\cdot yH_2O$, where M^{2+} and M^{3+} represent the divalent and trivalent cations in the octahedral sites within the hydroxyl layers and A^{n-} an exchangeable interlayer anion. The value of x indicates the level of representation of trivalent cations in the hydroxyl layers varying in the range of $0.25 \leq x \leq 0.33$ (if x is defined as $x = M^{3+}/(M^{2+} + M^{3+})$; the value of y indicating then the number of interlayer water molecules. Carbonates are the most frequently used interlayer anions that compensate the positive net charge of hydrotalcites. The hydrotalcite also contains the water of crystallization being situated in a free space of hydroxyl layers.

There were different types of the synthesis of Mg-Al mixed oxides reported and originating from the Mg-Al hydrotalcite-like precursors. The Mg-Al hydrotalcite materials have been prepared by precipitation [13], hydrothermal synthesis and treatments [14] or ion-exchange methods [15]. When using the precipitation method, it is necessary to apply the conditions of the so-called supersaturation in order to precipitate two or more cations.

Supersaturation conditions are usually attained by physical evaporation or, most often, chemical by pH-variation methods. Three of such methods based on co-precipitation have been reported, when the supersaturation conditions have been reached by:

- titration with NaOH [16],
- constant pH at low supersaturation; the pH value being controlled by simultaneously adding the solution containing M^{2+} and M^{3+} ions and the second one containing a base (KOH, NaOH, Na_2CO_3) in one container [8]. This method is the most frequently used for the Mg-Al hydrotalcite preparation. It was also selected in this work, where the pH value had been controlled by using the mixture of 0.5 M Na_2CO_3 + 3 M NaOH.

- constant pH at high supersaturation; two solutions with M^{2+} and M^{3+} ions being quickly added into the solution containing NaOH or Na_2CO_3 [17].

In this work, we focused on the comparison of structure and basic properties of Mg-Al mixed oxides prepared by two different types of synthesis. Of interest was the synthesis of Mg-Al mixed oxides with the different properties, as the application of Mg-Al mixed oxides in the individual catalytic reactions would require the different structure and basic properties. As the Mg/Al molar ratio is another parameter affecting the structure and basic properties of Mg-Al mixed oxides, we kept the same Mg/Al molar ratio (Mg/Al 2) in the case of the synthesized materials. Further, we selected the synthesis of Mg-Al mixed oxides based on the co-precipitation method, where the individual methods differ mainly in the application of alkaline solution used. We used two solutions: 0.5 mol l^{-1} Na_2CO_3 + 3 mol l^{-1} NaOH and 2 mol l^{-1} NaOH, respectively. Moreover, MgO and two Mg-Al mixed oxides available at large scale were used to compare the structure and basicity with those materials synthesized in the laboratory.

Experimental

Synthesis of Materials

MgO was supplied from Sigma-Aldrich. Two large-scale available hydrotalcite-like precursors were applied; the respective materials being denoted as HT-I and HT-II and the Mg-Al hydrotalcite as HT-III synthesised according to a procedure after Kovanda *et al*. [18]. An aqueous solution of $Mg(NO_3)_2 \cdot 6H_2O$ and $Al(NO_3)_3 \cdot 9H_2O$ (with the total metal ion concentration of 1 mol l^{-1}) was slowly added to 200 ml redistilled water. The flow rate of simultaneously added alkaline solution of Na_2CO_3 (0.5 mol l^{-1}) and NaOH (3 mol l^{-1}) was controlled to maintain the reaction conditions at desired pH of 9.5 ± 0.5. The co-precipitation was carried out under vigorous stirring (1 400 rpm) at 75 °C. The resulting suspension was then maintained at 75 °C and pH 9.5 ± 0.5 with stirring for 1 h. The product was filtered, washed several times with redistilled water to adjust the filtrate at pH > 7 and, finally, dried for 12 h at room temperature.

Mg-Al hydrotalcite denoted as HT-IV was synthesised according to Alvarez *et al*. [7]. An aqueous solution of $Mg(NO_3)_2 \cdot 6H_2O$ and $Al(NO_3)_3 \cdot 9H_2O$ with the total metal ion concentration of 1.0 mol l^{-1} was added dropwise into a glass vessel which had initially contained 200 ml redistilled water. The basicity was controlled by adding a solution of 2 M NaOH and kept at pH 10. Both solutions were vigorously mixed, when the suspension being stirred overnight at room temperature. The product was filtered, washed with redistilled water several times until the filtrate exhibited pH of about 7 and dried for 12 h at room temperature.

Mg-Al mixed oxides were obtained by calcination of hydrotalcite-like

materials, when the HT-I, -II, -III and -IV types were grain to 0.25-0.5 mm in particle size and calcined at 450 °C for 4 h in flow of air. The corresponding Mg-Al mixed oxides are denoted as Mg-Al-I, Mg-Al-II, Mg-Al-III and Mg-Al-IV, respectively.

Characterisation of Catalysts

XRF. The chemical composition of as-prepared samples was determined using XRF analysis, recorded with an X-ray fluorescence spectrometer (model PW1404, Philips).

BET. Specific surface areas (S_{BET}) of Mg-Al mixed oxides were measured at the boiling point of the liquid nitrogen (–196 °C) and determined by the fitting of the experimental data to the BET isotherm.

XRD. Powder X-ray diffraction (XRD) patterns were recorded with a diffractometer (AXS D8-Advance, Bruker) using the Cu K" radiation (λ = 0.154056 nm) with a secondary graphite monochromator. The coherence length in Mg-Al mixed oxides was calculated from the width of periclase (220) diffraction line (observed approximately at 62.5° 2θ) when using the Scherrer's equation ($D = K\lambda/\beta \cos\theta$), where D means the coherence length that characterises the crystallite size of MgO-like phase [nm], K is the shape factor (value of K = 0.9 was used), λ wavelength of X-ray radiation, β is FWHM (full width at half maximum) value [rad], and θ the diffraction angle [rad] [19].

TGA. Thermogravimetric analysis (TGA) of the Mg-Al hydrotalcites was performed using an equipment by TA Instruments TGA Discovery series operated at heating ramp of 10 °C min^{-1} from room temperature up to 900 °C in the nitrogen flow (20 ml min^{-1}, Linde 3.0). Twenty mg sample was heated in an open alumina crucible.

TPD-CO_2. Temperature programmed desorption of carbon dioxide as a probe molecule (TPD-CO_2) was carried out with the aid of Micromeritics device (model AutoChem 2920) equipped with a TCD detector and mass spectrometer with quadrupole analyser (MS OmniStar). A portion of 100 mg Mg-Al mixed oxide (grain of 0.25-0.5 mm) was placed in quartz reactor.

Before the TPD experiments, the samples were treated in the helium flow (25 ml min^{-1}) at 450 °C for 2 h, cooled down to 25 °C, and treated in a flow of 10 % CO_2/He (25 ml min^{-1}) for 60 min. To prepare this mixture, 99.99% CO_2 was used when being injected through the bed of sample till attaining the saturation. The excess of carbon dioxide was removed by flushing with helium at 25 °C for 30 min (25 ml min^{-1}). The desorption of CO_2 was measured by heating the sample from 25 to 700 °C at a heating rate of 10 °C min^{-1} in the flow of helium (25 ml min^{-1}). The desorbed products were analysed by the mass spectrometer. The number of basic sites was calculated from the CO_2 peaks (the molecular ion, m/z

= 44) with the aid of calibration for the known amount of CO_2 desorbed from the decomposed $NaHCO_3$.

Results and Discussion

Structure of Mg-Al Hydrotalcites and Mg-Al Mixed Oxides

Figure 1A shows the diffractograms of Mg-Al hydrotalcite-like materials. The diffraction lines at 11.6, 22.2, 34.2, 38.2, 45.1, 59.9 and 61.1° are typical of hydrotalcite-like structure exhibiting a specific double-layered structure of hydrotalcites [12,20]. The formation of other segregate phases (gibbsite $Al(OH)_3$) was observed only in the case of HT-II; i.e., in the large-scale material available for studies. Table I surveys the hydrotalcite lattice parameters *a* and *c* being calculated on the basis of d_{003} and d_{110} values that originated from the diffraction lines at 11.6 and 59.9° ($a = 2\ d_{110}$, $c = 3\ d_{003}$). The values *a* (cation-cation distance in the brucite-like layer) and *c* (thickness of one brucite-like layer and one interlayer) are in the range of that values reported for pure hydrotalcite phases [7,15]. All hydrotalcite-like materials exhibited approx. the same value of the unit cell dimension *a*. Usually, it is accepted that the unit cell dimension values (*a*) increases with the increasing Mg/Al molar ratio [7], which is consistent with the direct substitution of Al^{3+} (the ionic radius 0.53 Å) by Mg^{2+} (the ionic radius 0.72 Å) in the brucite-like layers [15]. Thus, the same values of unit cell dimension (*a*), being a function of cation-cation distance in the hydrotalcite layers support our assumption about the successful synthesis of Mg-Al hydrotalcite precursors with the almost same Mg/Al molar ratio. The parameter *c* is influenced by the size of the interlayer anion and the $Al^{3+} – Mg^{2+}$ cations. It has also been reported that this parameter increases with the increasing Al content. The parameter *c* was in the range of 22.80-23.32 Å for hydrotalcites in carbonate form (HT-I, -II and -III); i.e., in the range reported in literature [17,21]. On the other hand, HT-IV exhibited the value of parameter *c* 25.50 Å (Table I), which is a value higher compared to those observed for hydrotalcites in carbonate form. Finally, the value of parameter *c* is in agreement with the value of parameter *c* reported by Alvarez *et al*. [7] based on which the HT-IV materials have been synthesised.

Figure 1B shows the diffractograms of Mg-Al mixed oxides. It was found out that the diffractograms comprised two intense lines at 43.0° and 62.5° typical for the MgO-like phase or likely magnesia-alumina solid solution in Mg-Al mixed oxides [22,23]. Table II then gives a sight at the crystallite size of MgO calculated from the diffraction line at 62.5° by using the Scherrer's formula. The crystalline size of MgO decreased in the order: Mg-Al-III < Mg-Al-I < Mg-Al-IV < Mg-Al-II

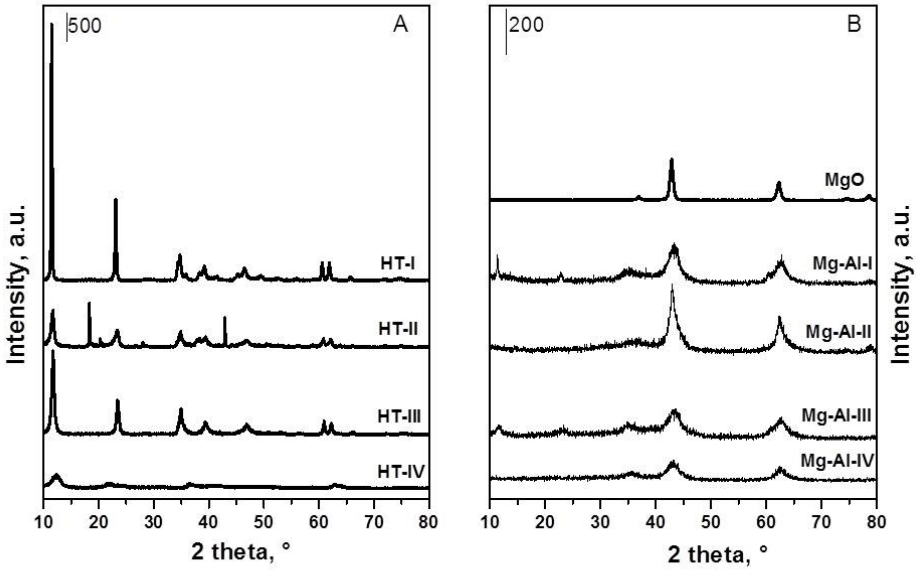

Fig. 1 Diffraction lines of Mg/Al hydrotalcites (A) and Mg-Al mixed oxides with the same Mg/Al molar ratio (B)

Table I List of Mg-Al hydrotalcites and their properties

	d_{003}, Å	a, Å	c, Å	Total mass loss (TGA), %
HT-I	7.77	3.056	23.32	45
HT-II	7.60	3.045	22.80	35
HT-III	7.61	3.044	22.84	43
HT-IV	8.50	3.050	25.50	46

<< MgO. Obviously, the crystalline size of MgO could be expected to be lower for laboratory synthesised Mg-Al mixed oxides (Mg-Al-III and Mg-Al-IV) in comparison with the large-scale available materials (Mg-Al-I and Mg-Al-II). Regarding this, the laboratory synthesised Mg-Al-III exhibited significantly lower MgO crystalline size than that for large-scale available Mg-Al-II. Nevertheless, the crystalline size of laboratory synthesised Mg-Al-IV was higher than Mg-Al-I prepared at large scale.

Figure 2 illustrates the TGA–DTA peaks obtained during the thermal analysis of the Mg-Al hydrotalcite-like materials. The character of these TGA had revealed a gradual weightloss process with two main events reflected as distinct peaks in the DTA (Differential Thermal Analysis). In general, for all hydrotalcites with the same molar ratio, the first step involves the loss of the interlayer water occurring between ambient temperature at about 125 °C. Dehydration takes place in two minor steps followed by a step at around 200 °C. The third step corresponded to the loss of OH^- groups and the decomposition of CO_3^{2-} in the layered double hydroxide structure. This process can be observed in the range of

380-400 °C [24]. In our case, the shapes of TGA curves and the positions of DTA peaks had demonstrated small differences among the individual materials. The similar shape of the TGA curves (Fig. 2) of all the samples suggests us their similar structure (XRD patterns of these LDH materials were also similar, see Fig. 1A). The differences were observed in the maxima of the DTA peaks, but the presence of maxima of the DTA peaks had still been in the range of values that corresponded to the above described processes. The total mass loss was found to be between 35 and 46 %.

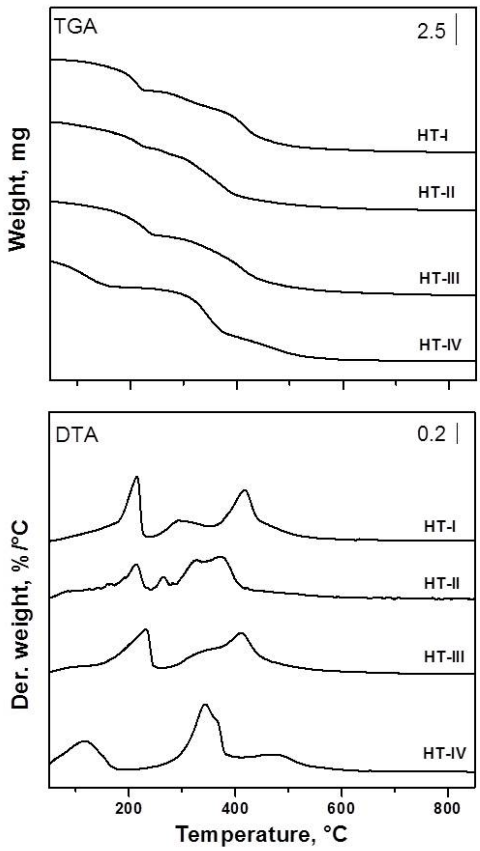

Fig. 2 TGA-DTA curves of Mg/Al hydrotalcite precursors

Basicity of Mg-Al Mixed Oxides

Determination of the concentration of the basic sites as well as the analysis of the amount of weak, medium, and strong basic sites in the Mg-Al mixed oxides are still under investigation and discussion. Most reported works have used the TPD-CO_2 as a powerful and relatively easy technique for determining the total concentration of basic sites. However, the results reported for TPD-CO_2 depend on experimental conditions; i.e., the purity and concentration of CO_2 during its adsorption (quoted to be 10 % CO_2/He), temperature of adsorption of CO_2 (from the room temperature up to 100 °C), the temperature, time, and flow of He used

for purging of the excess of CO_2 and the temperature gradient during desorption (5-20 °C min^{-1}). This is the reason, why the TPD profiles are not completely the same when comparing these experimental conditions in the individual laboratories.

Figure 3 shows TPD-CO_2 profiles of Mg-Al mixed oxides with Mg/Al molar ratio 2:1. The peak for desorption of CO_2 was observed between 50 °C and 475 °C. Such a region of desorption of CO_2 could be attributed to desorption of the gas from weak, medium, and strong basic sites [25,26]. The total concentration of basic sites (*CBS*) was calculated as the total amount of CO_2 desorbed between 50 °C and 475 °C; see Table II [21]. It is It is clearly seen that the concentration of basic sites depends on the type of the synthesis used. Total concentration of basic sites (*CBS*) decreased in order: Mg-Al-I (393 μmol g^{-1}) > Mg-Al-III (363 μmol g^{-1}) > Mg-Al-II (308 μmol g^{-1}) > Mg-Al-IV (222 μmol g^{-1}) >> MgO (99 μmol g^{-1}). Above 500 °C, the desorption of CO_2 is not connected with desorption from the basic sites, but originates from the residual amorphous $MgCO_3$ phase that had not been decomposed during the hydrotalcite thermal pre-treatment at 450 °C.

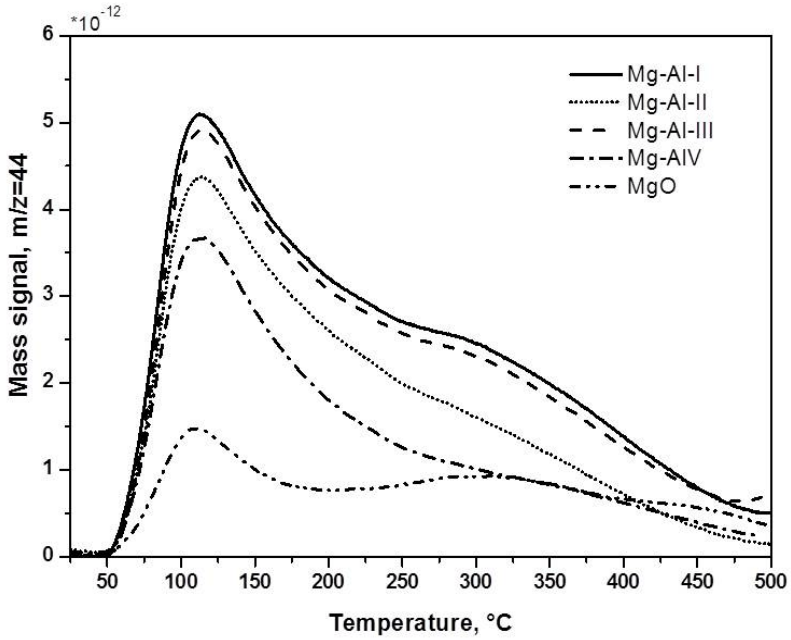

Fig. 3 TPD-CO_2 profiles of Mg-Al mixed oxides pre-treated at 450 °C

Mg-Al-IV mixed oxide was synthesised according to Alvarez *et al*. [7] who have reported on the presence of the two main desorption peaks at 111 and 540 °C in the TPD-CO_2 profile of the Mg-Al mixed oxide with Mg/Al 2. In our case, we observed the peaks for desorption of CO_2 at 95 and 295 °C in the TPD profile of Mg-Al-IV mixed oxide. Although we also noticed the desorption peak above 485 °C in the TPD-CO_2 profile of Mg-Al-IV, this peak could not be attributed to the desorption of CO_2 from the basic sites, but it has contributed to the release of CO_2 from the residual carbonate, remaining after calcination of the hydrotalcite-like

Table II List of Mg-Al mixed oxides and MgO, together with their properties

	Mg, wt. %	Al, wt. %	Mg / Al molar ratio	D(MgO) nm	S_{BET} $m^2\ g^{-1}$	CBS^* $\mu mol\ g^{-1}$
Mg-Al-I	37.2	20.0	2.1	3.0	200	393
Mg-Al-II	35.9	20.4	2.0	4.7	299	308
Mg-Al-III	35.3	21.5	1.8	2.7	191	363
Mg-Al-IV	34.4	22.4	1.7	3.4	-	222
MgO	-	-	-	10.8	111	99

* Total evolved amount of CO_2

precursor [10]. This nuance could be partially explained by the difference in the TPD experimental conditions as discussed above.

Although several authors have tried to separate the population basic sites of different strength by deconvolution of the TPD-CO_2 profile; for example, Carvalho *et al*. [26] and Grabowska *et al*. [27] used the Gaussian function for deconvolution of the TPD-CO_2 profile. Nevertheless, the utilization of Gaussian approximation is not the best solution in the case of TPD technique. In our case, we analysed the difference in the population of weak, medium, and strong basic sites at normalised TPD-CO_2 profiles.

Figure 4 depicts the normalised TPD-CO_2 profiles of Mg-Al mixed oxides with Mg/Al molar ratio 2:1 (as those shown in Fig. 3). Normalisation of the TPD profiles was done for the most intensive peak at 111 °C being the highest in all the TPD profiles. Figure 4 clearly documents the difference in the population of weak, medium, and strong basic sites, i.e., the different TPD profile. In literature, the presence of medium basic sites is being reported to be characteristic for the desorption peak at 140-170 °C [12,28,27], or at 220 °C [29], and the presence of strong basic sites reported to be typical for the desorption peak at 270-317 °C [12, 30,27], 400-450 °C [29] or 550-600 °C [31]. In our case, Figs 3 and 4 confirm only the presence of desorption peak at 95 and 295 °C. While desorption peak at 95 °C could easily be attributed to the presence of weak basic sites, it is hard to separate the medium and strong basic sites from the desorption peak at 295 °C and a shoulder of peak observed up to 500 °C.

At all the Mg-Al mixed oxides studied, the weak basic sites had represented the dominant type of basic sites. After that, the increasing intensity of desorption peak at 200-500 °C indicated the increasing ratio of the amount of medium and strong basic sites (desorption at 200-500 °C) to the amount of weak basic sites (the desorption peak at 95 °C). In this case, the intensity of desorption peak at 200-500 °C increased in the order: MgO > Mg-Al-I ~ Mg-Al-III > Mg-Al-II > Mg-Al-IV.

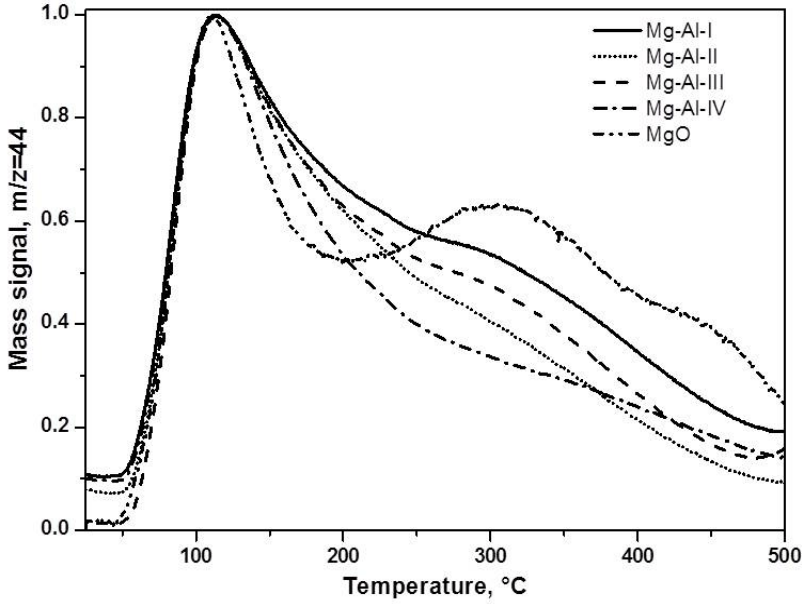

Fig. 4 Normalised TPD-CO_2 profiles of Mg-Al mixed oxides pre-treated at 450 °C

The Role of Basic Sites in Catalytic Reactions

Mg-Al-I, Mg-Al-II, Mg-Al-III and Mg-Al-IV mixed oxides represent the materials with approximately the same Mg/Al molar ratio (1.7-2.1, Table II), but the different and rather specific surface area (200-299 m^2 g^{-1}; Table II), the total concentration of basic sites (222-393 μmol g^{-1}, Table II) and the ratio between the population of medium/strong and weak basic sites (see Fig. 4). In contrast to Mg-Al mixed oxide materials, pure MgO exhibited the lowest amount of basic sites (CBS, Table II) but with the highest relative amount of medium/strong basic sites.

Laboratory synthesised Mg-Al-III mixed oxide, as well as both large-scale produced Mg-Al-I and Mg-Al-II materials, originated from hydrotalcite in the carbonate form. On the other hand, Mg-Al-IV mixed oxide was synthesised based on a procedure by Alvarez *et al*. [7], who had not used the carbonate solution during the hydrotalcite synthesis (but the solution of 2 M NaOH in order to keep the constant pH during the synthesis). The Mg-Al-IV mixed oxide contained the lowest total concentration of basic sites and the lowest relative amount of medium/strong basic sites in contrast to the mixed oxides originating from the hydrotalcites in the carbonate form.

In literature, the Mg-Al mixed oxides are mainly synthesised from the above mentioned hydrotalcites. Compared to the Mg-Al mixed oxides originating from hydrotalcites, we did not observe any extraordinary properties of the laboratory synthesised material (Mg-Al-III) and large scale of the materials available (Mg-Al-I and Mg-Al-II). Concerning the synthesis of such materials with large range of the amount of basic sites, there have already been the respective reports; namely, those

ones with the amount of basic sites: 170-330 μmol g^{-1} [32], 146-275 μmol g^{-1} [28], and 380-502 μmol g^{-1} [30]).

In contrast to that, the basicity was not reported for Mg-Al mixed oxides synthesised by that way as Alvarez *et al*. [7]. Although one could expect that the Mg-Al mixed oxides with higher amount of basic sites would be obtainable by modifying the conditions of synthesis; in our case, we synthesized the Mg-Al-IV mixed oxide with low value of basic sites as well as a low relative population of medium/strong basic sites. Such a type of basic properties could be powerful in the reactions, where Mg-Al mixed oxides are used as a support of the active component; e.g., in the selective oxidation of ammonia to elemental nitrogen catalysed by the Cu-Mg-Al and Fe-Mg-Al materials [33]. On the other hand, the synthesis of Mg-Al mixed oxides with the target concentration and the strength of basic sites is principal in other reactions, such as trans-esterification [34-36] and or Aldol condensation [37].

Conclusion

In this article, two different Mg-Al mixed oxides have been synthesized with approximately the same Mg/Al molar ratio (Mg/Al 2). Two large-scale available Mg-Al mixed oxides were used as reference materials. The structure and basicity of these materials were compared, ascertaining that the structure and the basicity significantly affect the catalytic behaviour of the Mg-Al mixed oxides in the individual reactions.

In contrast to Mg-Al mixed oxides originating from hydrotalcites in the carbonate forms (Mg-Al-I, -II and -III), the Mg-Al-IV mixed oxide (prepared by treating of hydrotalcite synthesised in concentrated NaOH solution) contained a lower total concentration of basic sites and lower relative population of medium/strong basic sites otherwise similar to the population of weak basic sites. It can be stated that such a type of basic properties could be powerful in the reactions, where Mg-Al mixed oxides are used as the support of the active component.

Acknowledgment

Authors would like to thank the ESF and the Ministry of Education, Youth and Sports of the Czech Republic, project CZ.1.07/2.3.00/30.0058 "Development of Research Teams at the University of Pardubice".

References

[1] Abelló S., Medina F., Tichit D., Perez-Ramírez J., Groen J.C., Sueiras J.E., Salagre P., Cesteros Y.: Chem.-Eur. J. **11**, 728 (2005).

[2] Liu Y., Lotero E., Goodwin J.G., Mo X.: App.l Catal. A-Gen. **331**, 138(2007).

[3] Prescott H.A., Li Z.J., Kemnitz E., Trunschke A., Deutsch J., Lieske H., Auroux A.: J. Catal. **234**, 119 (2005).

[4] Velu S., Swamy C.S.: Appl. Catal. A-Gen. **119**, 241 (1994).

[5] Climent M.J., Corma A., Iborra S., Primo J.: J. Catal. **151**, 60 (1995).

[6] Abelló S., Medina F., Tichit D., Pérez-Ramírez J., Sueiras J.E., Salagre P., Cesteros Y.: Appl. Catal. B-Environ. **70**, 577-(2007).

[7] Alvarez M.G., Chimentao R.J., Figueras F., Medina F.: Appl. Clay Sci. **58**, 16 (2012).

[8] Kustrowski P., Chmielarz L., Bozek E., Sawalha M., Roessner F.: Mater. Res. Bull. **39**, 263 (2004).

[9] Čapek L., Kutálek P., Smoláková L., Hájek M., Troppová I., Kubička D.: Top. Catal. **56**, 586 (2013).

[10] Garcia-Sancho C., Moreno-Tost R., Merida-Robles J.M., Santamaria-Gonzalez J., Jimenez-Lopez A., Torres P.M.: Catal. Today. **167**, 84 (2011).

[11] Kim M.J., Park S.M., Chang D.R., Seo G.: Fuel Process. Technol. **91**, 618 (2010).

[12] Di Cosimo J.I., Diez V.K., Xu M., Iglesia E., Apesteguia C.R.: J. Catal. **178**, 499 (1998).

[13] Mamhi A.J., Cosimo J.I.D., Apesteguia C.R.: in Cossio F., Bermúdez O., Angel G., Gomez R. (Eds), Proc XI IberoAmer. Symp. on Catalysis, IMP, Mexico D.F., **1**, 25 (1988).

[14] Budhysutanto W.N., Kramer H.J.M., van Agterveld D., Talma A.G., Jansens P.J.: Chem. Eng. Res. Des. **88**, 1445 (2010).

[15] Cavani F., Trifiro F., Vaccari A.: Catal. Today. **11**, 173 (1991).

[16] Ross G.J., Kodama H.: Amer. Min. **52**, 1037 (1967).

[17] Veloso C.O., Henriques C.A., Dias A.G., Monteiro J.L.F.: Catal. Today. **107**, 294 (2005).

[18] Kovanda F., Káfuňová E., Rojka T., Lang K.: Mater. Struct. **15**, 28 (2008).

[19] Jenkins R., Snyder R.L.: *Introduction to X-ray Powder Diffractometry*, John Wiley & Sons Inc. New York, 1996.

[20] Cantrell D.G., Gillie L.J., Lee A.F., Wilson K.: Appl. Catal. A-Gen. **287**, 183(2005).

[21] Perez C.N., Monteiro J.L.F., Nieto J.M.L., Henriques C.A.: Quim. Nova **32**, 2341(2009).

[22] Reichle W.T., Kang S.Y., Everhardt D.S.: J. Catal. **101**, 352 (1986).

[23] Constantino V.R.L., Pinnavaia T.J.: Inorg. Chem. **34**, 883(1995).

[24] Xu C.L., Gao Y., Liu X.H., Xin R.R., Wang Z.: Rsc. Adv. **3**, 793 (2013).
[25] Diez V.K., Apesteguia C.R., Di Cosimo J.I.: J. Catal. **215**, 220 (2003).
[26] Carvalho D.L., de Avillez R.R., Rodrigues M.T., Borges L.E.P., Appel L.G.: Appl. Catal. A-Gen. **415**, 96 (2012).
[27] Grabowska H., Zawadzki M., Syper L., Mista W.: Appl. Catal. A-Gen. **292**, 208 (2005).
[28] Bolognini M., Cavani F., Scagliarini D., Flego C., Perego C., Saba M.: Catal. Today. **75**, 103 (2002).
[29] Silva C.C.C.M., Ribeiro N.F.P., Souza M.M.V.M., Aranda D.A.G.: Fuel Process. Technol. **91**, 205 (2010).
[30] Veloso C.O., Perez C.N., de Souza B.M., Lima E.C., Dias A.G., Monteiro J.L.F., Henriques C.A.: Micropor. Mesopor. Mat. **107**, 23 (2008).
[31] Alvarez M.G., Segarra A.M., Contreras S., Sueiras J.E., Medina F., Figueras F.: Chem. Eng. J. **161**, 340 (2010).
[32] Di Cosimo J.I., Apesteguia C.R., Gines M.J.L., Iglesia E.: J. Catal. **190**, 261 (2000).
[33] Chmielarz L., Jablonska M., Struminski A., Piwowarska Z., Wegrzyn A., Witkowski S., Michalik M.: Appl. Catal. B-Environ. **130**, 152 (2013).
[34] Navajas A., Campo I., Arzamendi G., Hernandez W.Y., Bobadilla L.F., Centeno M.A., Odriozola J.A., Gandía L.M.: Appl. Catal. B-Environ. **100**, 299 (2010).
[35] Shumaker J.L., Crofcheck C., Tackett S.A., Santillan-Jimenez E., Morgan T., Ji Y., Crocker M., Toops T.J.: Appl. Catal. B-Environ. **82**, 120 (2008).
[36] Xie W.L., Peng H., Chen L.G.: J. Mol. Catal. A-Chem. **246**, 24 (2006).
[37] Hora L., Kelbichova V., Kikhtyanin O., Bortnovskiy O., Kubicka D.: Catal. Today. **223**, 138 (2014).